

# Time-division-multiplexing laser seeded amplification in a tapered amplifier

Wei Yang (杨威)<sup>1,2,3\*</sup>, Lin Zhou (周林)<sup>1,2</sup>, Shitong Long (龙世同)<sup>1,2,3</sup>,  
Wencui Peng (彭文翠)<sup>1,2,3</sup>, Jin Wang (王谨)<sup>1,2</sup>, and Mingsheng Zhan (詹明生)<sup>1,2</sup>

<sup>1</sup>State Key Laboratory of Magnetic and Atomic and Molecular Physics, Wuhan Institute of Physics and Mathematics, Chinese Academy of Sciences, Wuhan National Laboratory for Optoelectronics, Wuhan 430071, China

<sup>2</sup>Center for Cold Atom Physics, Chinese Academy of Sciences, Wuhan 430071, China

<sup>3</sup>University of Chinese Academy of Sciences, Beijing 100049, China

\*Corresponding author: yangwei@wipm.ac.cn

Received August 18, 2014; accepted November 14, 2014; posted online December 29, 2014

We demonstrate time-division-multiplexing (TDM) laser seeded optical amplification in a diode laser amplifier. With an acousto-optic modulator we combine two seeding beams of different frequencies and inject them alternately in the time domain into the tapered amplifier (TA) chip at a switching speed of 200 ns. The output high-power dual frequency components from the TA are time separated. The TDM seeded TA works safely and efficiently, which is useful for compact precision measurement instruments such as optical clocks and atom interferometers.

OCIS codes: 140.2020, 140.3280, 230.4110, 250.6715.  
doi: 10.3788/COL201513.011401.

In the field of optical communication, optical time-division-multiplexing (TDM) transmission technologies are essential in the construction of all-optical networks, which greatly improves the communication channel's transmission efficiency<sup>[1-4]</sup>. In the field of cold atom physics, we need a similar TDM technique. Examples demanding a TDM approach include not only transmitting laser beams with different frequencies and intensities in the same optical fiber in different time sequences to manipulate cold atoms but also using lasers efficiently and safely in constructing compact, sophisticated instruments that require stable and high laser power, and programmable control of timing sequences, such as optical atomic clocks<sup>[5]</sup> and atomic interferometers<sup>[6]</sup>. For example, in atomic interferometry experiments, we use several laser beams with different frequencies at different time sequences to cool and trap atoms in a magneto-optical trap, to launch an atom cloud by moving molasses, to manipulate atoms via two-photon stimulated Raman transition, to blow away the unwanted atoms, etc.<sup>[7,8]</sup>. In many cases we need not only just many lasers of different wavelengths at different time sequences but also high power, thus laser amplifiers are inevitably used. Tapered amplifiers (TAs) are widely used in cold atom experiments. Unfortunately a TA cannot amplify two frequencies simultaneously without interfering each other. Two-color operation normally causes mode competition and nonlinear mixing which generates unstable intensity and complicated laser components<sup>[9]</sup>.

Usually, two laser beams with different frequencies can be merged using a polarizing beam-splitting (PBS) cube, and then injected into the TA chip<sup>[10]</sup>. To ensure only one laser beam is injected into the TA chip

at specific time, shutters can be used to switch laser beams before they are superposed. However, independent control and running of the shutters may result in a mismatch of the two beams so that the TA chip will either be burned out with no input or be damaged by overloading. In addition, superposing two beams using a beam splitter with identical polarization loses about half of the beam intensity.

Here we propose a novel scheme to safely and efficiently operate amplifiers in the TDM mode, that is, using one amplifier to output different single-frequency lasers at different moments. We use a single acousto-optic modulator (AOM) to rapidly switch and combine two seed lasers alternately in the time domain while the TA is running. This allows one TA to amplify two single-frequency lasers to their maximum power in different time sequences. We demonstrate the feasibility and characterize the efficiency and switching speed of the TDM seeded TA.

The experimental scheme is shown in Fig. 1. Laser beams L1 and L2 are coupled via polarization-maintaining single-mode optical fibers. Before they enter the AOM, two half-wave plates (HWP1 and HWP2) are used to adjust the relative intensity of the two output beams of the PBS1, which ensure their power is equal. The mirror guarantees that L2 is well superposed on the negative first-order diffraction beam of L1. The two overlapping beams are coupled into the same optical fiber, and their polarization direction is adjusted by the HWP3. The fiber Port 4 on the other side collimates the output beams. The beams then pass through HWP4 and PBS2. The transmission beam is coupled into a TA chip (TA-0780-1000, m2k-laser) and the reflected beam is detected by a photodiode detector (Model 1621, New Focus),

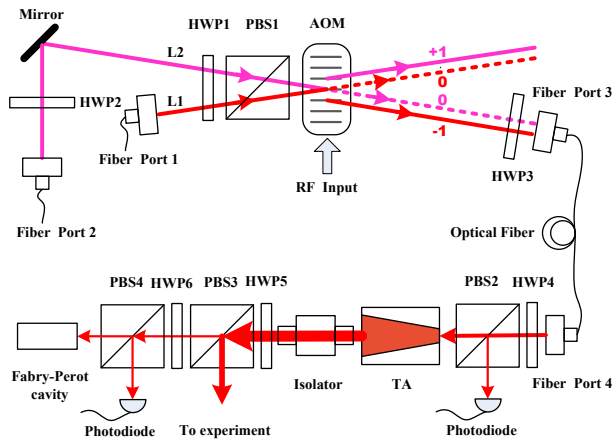


Fig. 1. (Color online) Schematic diagram of the experimental setup.

which monitors the switching process of the seed beams. The main part of the output beam of the TA is reflected by PBS3 for the main experiments and a small portion of the output passes through PBS3 for performance testing. The transmitted beam of PBS4 is analyzed using a free spectral range (FSR) Fabry–Perot cavity (Model 16P97, Coherent) to test the frequency components and the reflected beam of PBS4 is detected by another photodiode to monitor the power of the output. A Faraday optical isolator is used in the output side of TA to prevent back-reflection, and all optics on the output side are antireflection coated.

The main advantage of this configuration is that always only one beam is injected into the TA chip whenever the AOM is on or off, which efficiently protects the TA chip. Another advantage is that the switching speed of the AOM is very fast. Therefore the TA can keep running at its highest output power without worrying about overload or shutter failure.

The key feature of the device is dependent on the switching speed of the AOM<sup>[11]</sup>. The AOM is driven by a radio frequency (RF) source (DG4162, Rigol) and an amplifier (ZHL-2-8-S, Mini-Circuits). We can add lenses on either side of the AOM to correct the angular variation, but this will affect the diffraction efficiency and isolation of the two beams. To solve the problem, we selected the AOM with center frequency of 80 MHz (3080-125, Crystal) for higher diffraction efficiency, and employed the frequency shift keying (FSK) mode of the RF source to change the RF from 80 to 1 MHz, while keeping the input power of the RF signal constant. The 80 MHz AOM will not respond to the 1 MHz RF, thus giving no modulated output at this driving frequency end, or it operates as it is switched off. In this way we obtain a fast switch speed.

The two seed beams are obtained from external-cavity diode lasers operating at 780 nm, and the frequency difference between them is arbitrary. When the AOM is turned on, the negative first-order diffraction beam of L1 enters the fiber. Most of L2 is modulated in the positive

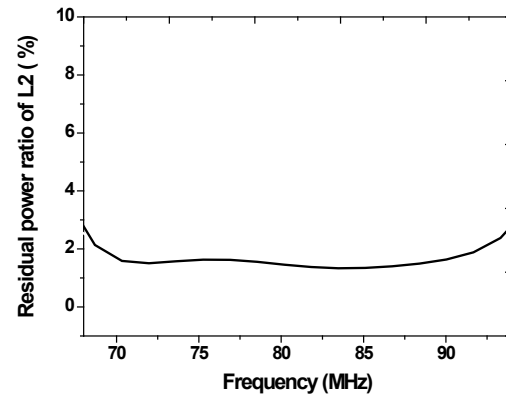


Fig. 2. Residual power ratio of the zero-order power  $P_0$  to the input power  $P_{L2}$  of L2 as a function of the RF when the RF is switched on.

first-order diffraction direction which is superposed on the zero-order beam of L1. However, there is some residual zero-order beam component of L2 still in the path of the negative first-order diffraction beam of L1, which also enters the fiber. Hence, we scan the frequency of the RF signal driving the AOM at around 80 MHz, detect the power of residual zero-order beam of L2, to find the best working point (Fig. 2). The result indicates that when the RF is set between 70 and 90 MHz, the residual power ratio of L2 ( $P_0/P_{L2}$ ) is lower than 2.0%, which corresponds to an isolation of 17 dB. The residual power at this level is very low so that it will not perturb the mode of output beam of the TA. This isolation is allowed in some experiments, such as the cooling process of atoms. If a higher purity of beam L1 is needed in the experiment, L2 can be shut off using other methods before it enters into the AOM to obtain a completely pure laser. On the other hand, when the AOM is turned off, only L2 enters into the fiber independently and we obtain a pure output laser, which can be used in processes such as atom interferometry.

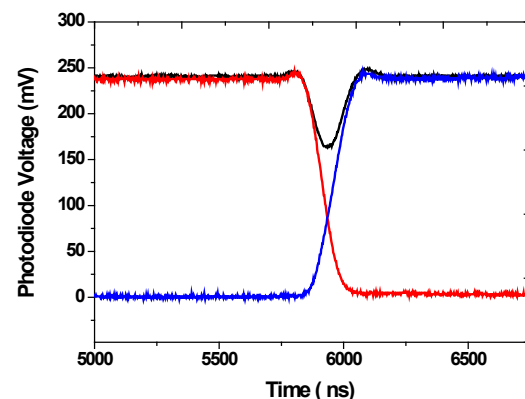


Fig. 3. (Color online) Power of the seed beams as a function of time during a switching on process. The blue curve shows the rising process of L1 detected after the optical fiber by the photodiode while L2 is blocked and the red one shows the falling process of L2 while L1 is blocked. The black curve is for the case that both L1 and L2 exist.

We measure the switching speed using a rapid response photodiode detector with a bandwidth of 1 GHz (Fig. 3). It shows the process of switching the AOM on and a similar figure can be obtained when the AOM is switched off. The color curves show the power increase in L1 and the power decrease in L2 when the AOM is turned on. The black curve shows the total power of the two beams. The result indicates that the switching time of the single beam with power from 10% to 90% is about 160 ns, which mainly depends on the time taken for the acoustic wave to transit across the laser beam waist. In our experiment, the beam waist is about 600  $\mu\text{m}$ , and the diffraction efficiency of the AOM and the coupling efficiency of the optical fiber are all optimum. However, when we switch the two beams, the total time is about 200 ns, which is 40 ns longer than switching a single beam, because we employ the FSK mode to switch the AOM. When the frequency is scanned from 1 to 80 MHz, the diffraction beam shifts from zero order to first order. We can detect a delay time of 40 ns in either diffraction direction. This results the total power of the two beams decrease about 30% during the switching process, and the zero-order and first-order diffraction beams increased equivalently. Since the TA can work in a pulsed current mode<sup>[12]</sup> and the switching time is in the nanosecond scale, this 200 ns switching time will not affect the operation of the TA.

We have tested the responses of the TA working in TDM mode, checking both the output power and the frequency. Firstly, we set the power of the two seed beams to be the same, and the total input power is lower than an accepted safe value to protect the TA chip. Two identical photodiode detectors are used to monitor the seed beams and the output beam of TA simultaneously. In Fig. 4, the red curve shows the intensity change of the input seed beams when we switch them and the black curve indicates the intensity response of the output beam from the TA. The result shows that the TA follows the change of the seed beam.

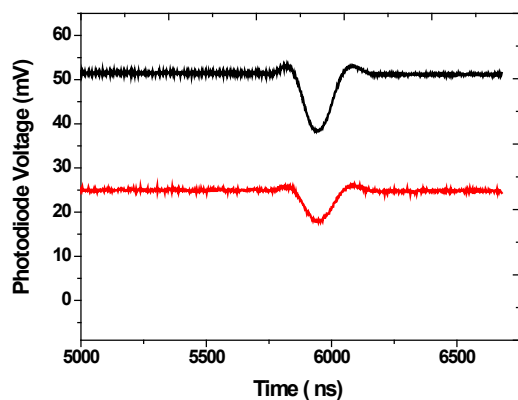


Fig. 4. (Color online) Response of the output beam of the TA (black curve) to the input seed beams (red curve) during switching process. This indicates that the TA follows the change in the seed beam.

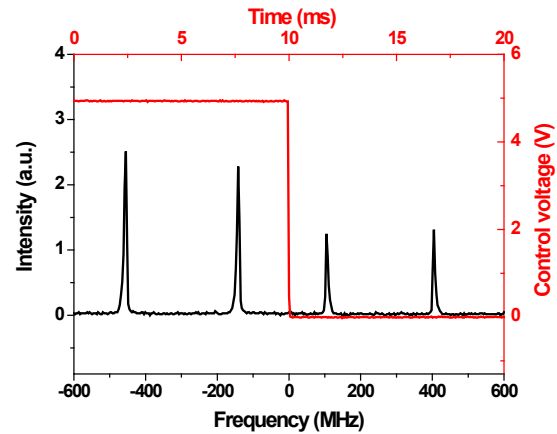


Fig. 5. (Color online) Response of output frequency of the TA before and after the seed beams are switched. The red curve is the one-period trigger signal of the spectral analyzer. The  $x$ -axis is calibrated using a single-frequency input, to ensure that a whole FSR is scanned.

Secondly, we use a Fabry-Perot spectral analyzer with a FSR of 300 MHz to analyze the frequency components of the output beam after the seed beam is swapped. The result is shown in Fig. 5. To see if there were any newly generated frequencies, we chose the frequency difference of the two seed beams not to be an integral multiple of the FSR. If there is more than one frequency component in the output beam, the spectrum can display the components by scanning one FSR. Meanwhile, the power of each seed beam is slightly adjusted to different values to distinguish the different frequency components. The result shows that there is only one output frequency component before and after switching the seed beam from one frequency to another. The contribution from the residual power of L2 does also appear in the signal, but the peak is small and cannot be seen obviously.

The above specifications of the TDM seeded TA mainly depend on the parameters of the AOM, for example, the insertion efficiency is more than 95%, the diffraction efficiency is more than 90% if the beam waist is 600  $\mu\text{m}$ , and the in-out isolation is 17 dB. The switching speed depends on the beam waist of the seed beams. The thinner the beam waist, the quicker the switching speed, but the lower the diffraction efficiency.

In conclusion, we demonstrate a rapid and efficient TDM scheme for the TA which can greatly improve its service efficiency. Although the TA is not conveniently used to amplify multiple frequencies simultaneously, they do work well in the TDM mode, and one TA can output multi-frequency lasers with maximum power in different time sequences. In addition, several TAs can be connected to efficiently manipulate laser beams with the same polarization direction.

This work was supported by the National Natural Science Foundation of China (Nos. 11227803 and 11204354), the National Basic Research Program of China

(No. 2010CB832805), and the funds from the Chinese Academy of Sciences.

## References

1. S. Kawanishi, *IEEE J. Quant. Electron.* **34**, 2064 (1998).
2. G. Liu, K. Y. Lee, and H. F. Jordan, *IEEE Trans. Comput.* **46**, 695 (1997).
3. H. G. Weber, R. Ludwig, S. Ferber, C. Schmidt-Langhorst, M. Kroh, V. Marembert, C. Boemer, and C. Schubert, *J. Lightw. Technol.* **23**, 225 (2005).
4. Y. Ji, X. Jia, Y. Li, J. Wu, and J. Lin, *Chin. Opt. Lett.* **11**, 050602 (2013).
5. L. Yu, Y. Li, J. Zang, D. Lu, B. Pan, and L. Zhao, *Chin. Opt. Lett.* **12**, 081402 (2014).
6. M. Kasevich and S. Chu, *Phys. Rev. Lett.* **67**, 181 (1991).
7. L. Zhou, Z. Xiong, W. Yang, B. Tang, W. Peng, Y. Wang, P. Xu, J. Wang, and M. Zhan, *Chin. Phys. Lett.* **28**, 013701 (2011).
8. L. Zhou, Z. Xiong, W. Yang, B. Tang, W. Peng, K. Hao, R. Li, M. Liu, J. Wang, and M. Zhan, *Gen. Relativ. Gravit.* **43**, 1931 (2011).
9. H. Luo, K. Li, D. Zhang, T. Gao, and K. Jiang, *Opt. Lett.* **38**, 1161 (2013).
10. G. Ferrari, M. Mewes, F. Schreck, and C. Salomon, *Opt. Lett.* **24**, 151 (1999).
11. W. Schwenger and J. Higbie, *Rev. Sci. Instrum.* **83**, 083110 (2012).
12. K. Takase, J. Stockton, and M. Kasevich, *Opt. Lett.* **32**, 2617 (2007).